IR783 Encapsulated in TR-conjugated Liposomes for Enhancing NIR Imaging-guided Photothermal and Photodynamic Therapy

Jiajia Lv
Zunyi Medical University
Tianjiao Luan
Zunyi Medical University
Mingyan Yang
Zunyi Medical University
Mengmeng Wang
Zunyi Medical University
Jie Gao
Zunyi Medical University
Zeli Yuan (zlyuan@zmu.edu.cn)
Zunyi Medical University https://orcid.org/0000-0001-5354-769X

Research Article

Keywords: liposome, RGD peptide, photothermal therapy, photodynamic therapy, NIR imaging guided

Posted Date: November 9th, 2021

DOI: https://doi.org/10.21203/rs.3.rs-1033993/v1

IR783 encapsulated in TR-conjugated liposomes for enhancing NIR imaging-guided photothermal and photodynamic therapy

Jiajia Lv[1,2,3,4], Tianjiao Luan[1,2,3,4], Mingyan Yang[1,2,3,4], Mengmeng Wang[1,2,3,4], Jie Gao[1,2,3,4*], Zeli Yuan[1,2,3,4*]

Abstract

We developed an integrin αvβ3-specific liposomes, TR-conjugated liposomes (TR-LPs), loading IR783 for NIR imaging-guided both PTT and PDT. The TR-LPs was composed of soyabeanphosphatidylcholine, cholesterol, 1,2-distearoyl-sn-glycero-3-phosphoethanolamine- N-[methoxy(polyethylene glycol)-2000] (DSPE-PEG) and TR-functionalized DSPE-PEG. IR783, NIR PTT/PDT diagnostic agents, were encapsulated in the hydrophilic core of the TR-LPs. DSPE-PEG had ability of reducing the absorption of TR-LPs by the reticuloendothelial system and increase the cycle time in body. RGD fragment on the TR peptide (TR = c(RGD)-AGYLLGHINLHHLAHL(Aib)HHIL-cys) enhanced the tumor selectivity of liposomes by specifically targeting integrin αvβ3-overexpressing cancer cells. Simultaneously, the rest of fragment on the TR peptide can be changed to the positive charge in the tumor microenvironment (pH 6.5), improving cellular uptake of photoagents at tumor site. We executed a set of in vitro and in vivo experiments to verify if, by functionalizing liposomes with an integrin αvβ3-specific and pH responding peptide, it is possible to achieve NIR imaging guided PTT/PDT for tumor treatment. TR-conjugated liposomes exhibited favorable physical and chemical stability, loading capacity, biocompatibility and tumor targeting. TR-LPs can safely and efficiently delivery IR783 to tumor sites to achieve their therapeutic function. IR783-TR-LPs is promising as a potentially safe and effective phototherapeutic agents for NIR fluorescence-guided tumor therapy applications.

Keywords: liposome, RGD peptide, photothermal therapy, photodynamic therapy, NIR imaging-guided

Background

Currently, phototherapy advancements have gradually shifted from monotherapy to multimodal therapy, typically combining photodynamic therapy (PDT) and photothermal therapy (PTT) into one system [1–6]. PDT mainly relies on photosensitizers (PS) under light irradiation to directly generate reactive oxygen species (ROS) to kill cells, so suitable irradiation wavelength and effective PS delivery is crucial to achieving excellent PDT efficacy [7]. PTT can not only generate hyperthermia to kill cancer cells, but also increase the saturated oxygen concentration and the amount of drug delivered by accelerating blood flow [8, 9]. Typically, hyperthermia is able to enhance the absorption of PS by promoting the permeability of cell membrane, and finally increase the concentration of PS in cancer cells [6]. More importantly, phototherapy can achieve fluorescence navigation to accurately activate PTT and PDT at tumor tissue and avoid normal tissue damage. Therefore, the combination of fluorescence imaging-guided PTT and PDT is a promising non-invasive method for cancer treatment.

The common method for developing multimodal phototherapy is mainly loading two or more PDT and PTT agents in one nanosystem. The strategy may face the following issues: (1) different lasers to activate treatment resulting complicated operation, device/time cost, synergistic therapeutic destruction, (2) complex preparation, and (3) challenges in obtaining optimal ratio of PTT and PDT agents to achieving synergistic effects. If both PDT and PPT agents can be activated simultaneously by the same light irradiation, it will unify the treatment time of PDT and PTT, reduce the complexity of treatment, as well as be more conducive to achieving optimal synergy. Thus, it is critical to develop a mono-phototherapy agent combing PTT and PDT that can simultaneously perform tumor-specific targeting, real-time fluorescence tracking in *vivo* and selective tumor ablation.

Near-infrared (NIR) irradiation and fluorescence imaging as emerging treatment technologies have used in fundamental research and clinical application, for the advances in increasing issue penetration depth, reducing tissue absorption, photon scattering, and tissue autofluorescence interference [10]. Owing to advances in excellent biodegradability, biocompatibility and low

toxicity, NIR organic dyes have received extensive attention. Indocyanine green (ICG), as an important derivative of cyanine dye, has been approved by the FDA for medical imaging in clinical practice. Therefore, many NIR fluorescent dyes studied are based on cyanine dye family. In addition to NIR fluorescence imaging, ICG is proven to have PTT and PDT capabilities [11]. However, since ICG is unstable in an aqueous medium and the fluorescence quantum yield is relatively low, which significantly reduces its imaging and therapy potential. Thus, various cyanine dyes were developed to improve the stability and photophysical properties of ICG. One of these strategies is the introduction of a rigid group in the middle of cyanine dyes, which can greatly improve the photophysical properties of cyanine dyes [12]. Typically, IR783 with a rigid carbocyclic ring exhibits that preferable aqueous stability and fluorescence quantum yield in comparison to ICG. IR783, a water-soluble cyanine dye, often demonstrates similar biodistribution profile to ICG after systemic administration and rapid clearance from systemic circulation [13]. IR783 is characterized by a short tumor retention time due to its rapid clearance, which greatly limits the time window in which phototherapy can be administered.

Liposomes, as the most successful nanocarrier in clinical applications, have been applied to a variety of commercial nanomedicines including Doxil, Caelyx and so all [14]. Although traditional liposomes have an enhanced permeability and retention (EPR) effect, the amount of enrichment at the tumor site is still limited. Recently, RGD (Arg-Gly-Asp) peptide functionalized liposomes is use to improve their tumor targeting due to the excellent specificity of RGD for αvβ3 integrin positive cells and tumor angiogenic vessels [15, 16]. He and co-workers developed integrin αvβ3-specific liposomes which respond to pH and cross the blood-brain barrier to treat glioma [17]. Gu and co-workers used quantum dots and RGD-functionalized polyethylene glycol (PEG) to construct sub-50 nm nanoparticles for inhibition of both primary and metastatic cancer [18]. Lin and co-workers designed a multimodal diagnostic nanoplatform for pohotothermal-enhanced chemotherapy of tumor, which was composed RGD peptide, melanin-coated magnetic nanoparticles, doxorubicin, and ICG [19].

In this work, we developed an integrin αvβ3-specific liposomes, TR-conjugated liposomes (TR-LPs), loading IR783 for NIR imaging-guided both PTT and PDT. The TR-LPs was composed

of soyabeanphosphatidylcholine (SPC), cholesterol (Cho), 1,2-distearoyl-sn-glycero-3-phosphoethanolamine-N-[methoxy(polyethylene glycol)-2000] (DSPE-PEG) and TR-functionalized DSPE-PEG. IR783, NIR PTT/PDT diagnostic agents, were encapsulated in the hydrophilic core of the TR-LPs. DSPE-PEG can reduce the absorption of TR-LPs by the reticuloendothelial system and increase the cycle time in body. RGD fragment on the TR peptide (TR = c(RGD)-AGYLLGHINLHHLAHL(Aib)HHIL-cys) enhanced the tumor selectivity of liposomes by specifically targeting integrin αvβ3-overexpressing cancer cells. Simultaneously, the rest of fragment on the TR peptide can be changed to the positive charge in the tumor microenvironment (pH 6.5), improving cellular uptake of photoagents at tumor site. We executed a set of in *vivo* and in *vivo* experiments to verify if, by functionalizing liposomes with an integrin αvβ3-specific and pH responding peptide, it is possible to achieve NIR imaging guided PTT/PDT for tumor treatment.

Results and discussion

Preparation and characterization of IR783-TR-LPs

IR783-TR-LPs were composed of SPC, Cho, DSPE-PEG and TR-DSPE-PEG. The IR783 were encapsulated in the hydrophilic core of the liposome nanoparticles (**Scheme 1**). DSPE-PEG had ability of reducing the absorption of IR783-TR-LPs by the reticuloendothelial system and increase the cycle time in body. Moreover, RGD fragment on TR peptide enhanced the specific targeting of liposomes to cancer cells overexpressing integrin αvβ3. Simultaneously, the rest of fragment on the TR peptide can be changed to the positive charge in the tumor microenvironment, improving cellular uptake of liposomes at tumor site [17].

As presented in **Fig. 1** and **Table 1**, the hydrodynamic size of the TR-LPs was measured to be 104.4 nm at pH 6.5 and 143.3 nm at pH 7.4. The reduction in particle size of the TR-LPs at pH 6.5 will facilitate tissue penetration [20]. Compared to TR-LPs, PEG-LPs had no change in the hydrodynamic size at pH 6.5 and 7.4. In addition, encapsulation efficiency of TR-LPs was calculated to be 19.0%, and the IR783 loading content was about 11.2%, which was capable of acting as a nanovehicle for loading IR783. Furthermore, the zeta potential of TR-LPs and PEG-LPs was analyzed by a Zeta PALS instrument. The PEG-TPs possessed a negative surface

potential of −18.15 mV at pH 6.5 and −16.00 mV at pH 7.4. After assembling with TR-DSPE-PEG, the zeta potential rose to −7.83 mV at pH 7.4. At pH 6.5, TR-DSPE-PEG significantly enhanced the surface potential of TR-LPs, which was measured to be +5.09 mV. The change of zeta potential showed that TR-LPs could undergo charge reversal (the zeta potential changing from negative to positive) under slightly acidic conditions, which was beneficial to cellular uptake in tumor microenvironment.

For subsequent biological applications, we investigated the stability of TR-LPs and PEG-LPs in PBS (pH 7.4), DMEM and 10% FBS (FBS:PBS, v:v) by DLS (**Fig. 1C** and **Fig. S1**). The particle size of TR-LPs fell in the range of about 110 nm without significant change in three different media for 24 hours. Similarly, the particle size of PEG-TPs was relatively stable in these three solutions for 24 hours. Finally, TR-LPs and PEG-LPs presented stability in PBS, DMEM and 10% FBS with no precipitation stored in dark, and 4 °C for storing at least one week.

As shown in **Fig. 1D**, UV-Vis spectra showed that free IR783 possessed a strong absorption peak at ~776 nm in PBS. After IR783 encapsulated, the absorption spectrums of IR783-TR-LPs and IR783-PEG-LPs had almost no change compared with free IR783. If the IR783 located in a hydrophobic area of liposomes, its spectral absorption may change significantly due to changes in solvent polarity. Furthermore, the absorbance spectrums of TR-LPs and PEG-LPs possessed the characteristic peaks of IR783 with minor changes, illustrating that IR783 had been successfully encapsulated and located at hydrophilic core of the liposome nanoparticles.

Free IR783, IR783-PEG-LPs and IR783-TR-LPs were separately stored under irradiation of LED light (white light, 6.78 W) at room temperature to investigate the photostability of them. The UV-Vis spectra of free IR783, IR783-PEG-LPs and IR783-TR-LPs were recorded at a specific time point for 47 min. Finally, the half-life ($t_{1/2}$) of free IR783, IR783-PEG-LPs and IR783-TR-LPs were 12.6 min, 14.2 min and 16.4 min by fitting the maximum absorbance IR783 (**Fig. 1E**). Obviously, IR783-TR-LPs showed better stability than IR783-PEG-LPs and free IR783. Thus, the relative photostability of IR783-TR-LPs was helpful for subsequent experiments in vitro and in vivo.

In the release experiment of IR783, IR783-TR-LPs exhibited more cumulative release of IR783 at pH 6.5 (68.2%) than that of pH 7.4 (55.0%) after 24 h (**Fig. 1F** and **Fig. S2**). IR783, being both a photothermal and a photodynamic agent, its ability to be released from liposomes did not affect its ability to exert phototherapeutic effects in our system. Ultimately, That the ability of IR783 loading with above liposomes to achieve maximum enrichment at the tumor site is key to achieving optimal PTT/PDT effects.

Phototheranostic properties

To achieve optimal imaging and therapeutic results in *vivo*, it is critical that IR783 has good photophysical properties in NIR region. IR783, as cyanine dye-based phototheranostic agents, dissolved in PBS buffer exhibit NIR maximum absorption (~776 nm) and fluorescence emission (~794 nm). Fluorescence quantum yields (Φ_F) for IR783-TR-LPs and IR783-PEG-LPs were calculated in PBS buffer using IR783 as the reference (Φ_F was 18.6% in PBS buffer, pH 7.4) [21]. Fluorescence quantum yields of the formulated IR783-TR-LPs and IR783-PEG-LPs were 17.2% and 16.9%, while maintaining phototherapeutic abilities. Noteworthy, Φ_F of IR783-TR-LPs and IR783-TR-LPs was reduced to 7.5% and 9.1%, presumably due to aggregation of IR783 in the hydrophilic core of the liposomes resulting fluorescence quenching effect.

To assess photothermal properties of the free IR783, IR783-TR-LPs and IR783-PEG-LPs in PBS buffer at different IR783 concentration (0, 0.25, 0.5, 1 mM) exposed to NIR laser light (808 nm, 2 W/cm^2) or at the same IR783 concentration (0.5 mM) exposed to laser irradiation (0, 1, 2, 3 W/cm^2) for 10 min and temperature profiles were obtained (**Fig. 2A, 2B and Fig. S3**). The results revealed that IR783, the free IR783, IR783-TR-LPs and IR783-TR-LPs (at different IR783 concentration) all exhibited a rapid increase in temperature during exposure to NIR laser light (808 nm, 2 W/cm^2), reaching about 50°C at 400 s. Then, the temperature remained at 50°C for the next 200 s and did not continue to rise. This was caused by the gradual photodegradation of IR783, and it was also observed that the solution gradually changed from dark green to brown in experiments. Finally, the photostability of IR783-TR-LPs, IR783-PEG-LPs and free IR783 was also investigated. Toward this end, free IR783 and IR783 loaded by two liposomes were subject to repeated irradiation–cooling cycles using 808 nm laser irradiation (2 W/cm^2) for 140 min

followed by passive cooling to room temperature. As shown in **Fig. 2C, 2D and Fig. S4**, the variation in the maximal temperature increased during the whole cycle proved to be 1.9%, leading us to conclude that only IR783-TR-LPs was stable under conditions of 808 nm laser irradiation. In contrast, the maximum temperature of PEG dropped significantly (from 74°C to 65.7°C) in final irradiation cycle. After the fourth irradiation cycle of free IR783, the maximum temperature continued to drop (73.6°C $\rightarrow$53.2°C$\rightarrow$25.8°C), and the temperature can no longer rise in the last cycle. These results proved that TR-LPs and PEG-LPs could protect IR783 from photobleaching, which was consistent with the previous experiment on stability of white light irradiation at room temperature.

In addition to the above optical and photothermal properties, the ROS generation of IR783 was also measured. After exposure to an 808 nm laser (0.5 W/cm^2) for 100 s, IR783 capable of generating ROS, with respect to the dark controls and ROS scavenger (**Fig. 2E**).

Based on the above results, we selected IR783-TR-LPs, IR783-PEG-LPs and free IR783 for subsequent studies in *vitro* and in *vivo*. The above two liposomes (PEG-LPs and TR-LPs) both demonstrated enhanced photophysical and phototherapeutic properties compared to free IR783.

In *vitro* phototherapy evaluation

To demonstrate phototheranostic efficacy of IR783-TR-LPs, a 4T1 breast cancer cell line was used for in *vitro* studies. Upon exposure to 808 nm laser irradiation, Intracellular ROS generation of the IR783-TR-LPs, IR783-PEG-LPs and free IR783 can detect by DCFH-DA, which exhibit green fluorescence in 4T1 cells. As shown in **Fig. 3A**, the 4T1 cells treated by IR783-TR-LPs, IR783-PEG-LPs and free IR783 with NIR irradiation exhibit green fluorescence, demonstrating an amount of ROS generation in cells. Moreover, IR783-TR-LPs showed slightly higher fluorescence intensity and produces more ROS, which is consistent with the results of cell imaging. No fluorescence can be found in cells treated by the control groups of "no irradiation", "addition of N-acetylcysteine with 808 nm laser irradiation", "cells treated with DCFH-DA under irradiation", "cells treated with DCFH-DA in dark", and "PBS".

Furthermore, in *vitro* PDT/PTT efficiency of IR783-TR-LPs, IR783-PEG-LPs and free IR783 in 4T1 cells was investigated by MTT assay. Two different power of laser (800 nm, 0.1 and 0.5

W/cm^2) irradiating for 2 minutes were examined at the fixed concentration of IR783 (10 μM) in different pH (pH 7.4 and pH 6.5) (**Fig. 3B and 3C**). Under the same pH conditions, the cell viability of IR783-TR-LPs was the lowest among the experimental groups after different power illumination. At pH 6.5, IR783-TR-LPs showed a better phototherapy effect. This is due to the encapsulation of free IR783, which enhanced the cell uptake and phototherapy of IR783. These results demonstrated that IR783-TR-LPs with NIR laser had ability of effectively killing tumor cells. According to the results of dark toxicity experiments (**Fig. S5**), the free IR783 was not toxic in the experimental concentration range, indicating good biocompatibility for subsequent cellular and in *vivo* applications.

In *vivo* imaging and phototheranostic study

To evaluate the tumor targeting ability of IR783-TR-LPs, the in *vivo* biodistribution of IR783-TR-LPs, IR783-PEG-LPs and free IR783 after tail vein injection were performed on BALB/c mice bearing 4T1 tumor by a small animal NIR-imaging system. IR783-TR-LPs presented a much stronger NIR-fluorescence signal in the tumor site at 8 h and 24 h compared with IR783-PEG-LPs, which further demonstrated that TR ligand could effectively promote IR783 accumulating in the tumor region in *vivo* (**Fig. 4A**). For IR783-TR-LPs, IR783 was predominantly cleared from the tumor and body within 48 h. Compared with IR783-TR-LPs and IR783-PEG-LPs, free IR783 also exhibited the property of preferential accumulation at the tumor area despite weaker fluorescence intensity. Distinguished accumulation of free IR783 in the tumor was observed at 2 h until at 8 h post injection, and IR783 was quickly cleared from the tumor and body within 24 h. The results of fluorescence imaging suggested that 8 h post injection was the optimal temporal window for phototherapy.

Afterward, the major organs (heart, liver, spleen, lung and kidney) and tumor of BALB/c mice were collected for ex *vivo* imaging at 8 h. The fluorescence signal of IR783-TR-LPs group at the tumor region was significantly higher than that of IR783-PEG-LPs and free IR783 group (**Fig. 4A**), which was nearly quadruple and fifteen times using quantitative region-of-interest analysis, respectively (**Fig. S6**). In addition, the fluorescence signal at the tumor site was approximately double than that in liver or kidney after injection of IR783-TR-LPs after 8 h.

As presented in **Fig. 4B**, the tumor temperature of IR783-TR-LPs group at 8 h post injection elevated quickly from 30.3 °C to 41.3 °C with laser irradiation (808 nm, 0.5 W/cm^2) for 1 min. However, IR783-PEG-LPs and free IR783 groups showed a relatively slight increase. Moreover, the tumor temperature of IR783-TR-LPs group increased to 42.0 °C after laser irradiation for 5 min, which was higher than that of both IR783-PEG-LPs group (41.1 °C) and free IR783 (39.5 °C). As a control, the tumor temperature of PBS group was increased from 30.7 °C to 37.7 °C after laser irradiation for 5 min. These results are also consistent with the results of NIR imaging, demonstrating the effectiveness of NIR imaging-guided phototherapy. Thus, IR783-TR-LPs had the potential to be a promising NIR imaging-guided PDT/PTT agent for tumor treatment applications.

Encouraged by the high enrichment of IR783 from IR783-TR-LPs in tumor regions, we next studied both PDT and PTT efficiency in *vivo*. 4T1 tumor-bearing mice were tail-vein injected with IR783-TR-LPs, IR783-PEG-LPs and free IR783 (1 mg/kg of IR783). In *vivo* study, 4T1 tumor-bearing mice were randomly divided into four groups of five mice each, denoted as “IR783-TR-LPs”, “IR783-PEG-LPs”, “free IR783” and “PBS”. According to the results of NIR and photothermal imaging, the optimal therapeutic windows was determined at 8 h after injection for 5 min. Subsequently, All mice of four groups were exposed by 808 nm laser (0.5 W/cm^2) at 8 h after injection for 5 min. The in *vivo* antitumor effects of the above photoagents were investigated by monitoring the changes in tumor volume for 15 days. As shown in **Fig. 5A**, the inhibition of tumor growth by treatment in the PBS group was negligible, indicating that 808 nm laser irradiation alone did not have an anti-tumor effect. It was revealed that treatment in “free IR783” group and “IR783-PEG-LPs” group can inhibit the tumor growth to some degree due to both PDT and PTT of free IR783, in spite that the average tumor volume on day 15 was around 8 times larger than that on day 0. Unexpectedly, “IR783-TR-LPs” group after treatment revealed the most effective antitumor activity, as demonstrated by slow tumor growth at day 15. Tumor photographs further confirmed the optimal anti-tumor activity of the “IR783-TR-LPs” group, providing visual evidence (**Fig. 5B**). In addition, negligible weight loss was observed in four groups of mice, indicating low in *vivo* toxicity of the photo-treatments (**Fig. 5C**), which were further supported by

the hematoxylin and eosin (H&E) staining of liver and kidney tissues from all groups of each mouse, indicating the absence of significant lesions in normal organs (**Fig. S7**). On the 15th day, all four groups of mice were sacrificed to collect the tumor tissues, then sliced and stained with H&E and TUNEL (in situ terminal deoxynucleotidyl transferased dUTP nick end labeling). The images histological sections demonstrate that among the different therapeutic agents, "IR783-TR-LPs" group the most effective antitumor effect causing tumor necrosis, inducing apoptosis and hindering the proliferation of cancer cells (**Fig. 5D**). Additionally, the PEG-LPs and TR-LPs did not cause hemolysis in treatment (**Fig. S8 and S9**).

Conclusion

In summary (**Figure 6**), we have developed a versatile facile phototheranostic nanoagent based on TR-conjugated liposomes loading IR783 for enhancing NIR imaging-guided PTT and PDT. TR-conjugated liposomes exhibited favorable physical and chemical stability, loading capacity, biocompatibility and tumor targeting. Guided by NIR fluorescence of IR783, we visualized the tumor by NIR fluorescence in *vivo* to investigate the optimal time of IR783 enrichment and finally achieved the optimal both PTT and PTT effect using NIR laser. As a comparison to both IR783-PEG-LPs and free IR783, IR783-TR-LPs show the best treatment effect. These results clearly indicate that TR-LPs, as a liposome, can safely and efficiently delivery IR783 to tumor sites to achieve their therapeutic function. Meanwhile, with the help of TR-LPs, the physical and chemical properties of IR783 were not only improved, but also its tumor selectivity was enhanced. IR783-TR-LPs is promising as a potentially safe and effective phototherapeutic nanoagent for fluorescence-guided tumor therapy applications. The above study is only as a proof of concept. In the future, TR-LPs can be applied not only to load more other drugs than just photoagents to achieve specific recognition of tumor cells, but even replace TR peptides with other targeting molecules functionalized liposomes for achieving a wider range of medical applications.

Material and methods

Materials

Soyabeanphosphatidylcholine (SPC), cholesterol (Cho), IR783 (2-[2-[2-Chloro-3-[2-[1,3-dihydro-3,3-dimethyl-1-(4-sulfobutyl)-2H-indol-2-ylidene]ethylidene]-1-cyclohexen-1-yl]ethenyl]-3,3-dimethyl-1-(4-sulfobutyl)-3H-indolium inner salt sodium salt), 1,3-diphenylisobenzofuran (DPBF) were purchased from Sigma-Aldrich. 1,2-distearoyl-sn-glycero-3-phosphoethanolamine-N-[methoxy(polyethylene glycol)-2000] (DSPE-PEG) was obtained from Avanti Polar Lipids. TR-DSPE-PEG (TR = c(RGD)-AGYLLGHINLHHLAHL(Aib)HHIL-cys) was obtained from Xi'an ruxi Biological Technology. Cytiva illustra NAP-25 columns were purchased from GE Healthcare.

Preparation of IR783-PEG-LPs and IR783-TR-LPs

IR783-PEG-LPs and IR783-TR-LPs were assembled via thin film dispersion. Take the preparation of IR783-TR-LPs as an example, SPC, Cho, DSPE-PEG and DSPE-PEG-TR (59:33:2:6, n:n:n:n) were dissolved in mixtures of chloroform and methanol (2:1, v:v). A thin lipid film was formed by evaporating with a stream of nitrogen and drying overnight under vacuum to avoid residual organic solvents. Then, the thin lipid film was rehydrated with 1 mL of IR783 solution (30 mM, 10 mM HEPES buffer, pH 7.4), agitation at room temperature for 30 min and sonication at –4°C for 5 min. Extravesicular components were removed by Sephadex G-25 chromatography (NAP-25 column) with 10 mM HEPES buffer, pH 7.4. Except no DSPE-PEG-TR was added, the preparation of IR783-PEG-LPs was similar to the above methods.

Characterization of IR783-PEG-LPs and IR783-TR-LPs

The hydration diameter, polydispersity, and zeta potential of IR783-PEG-LPs and IR783-TR-LPs were investigated using dynamic light scattering (DLS) measurements performed on NanoBrook 173plus equipped with a digital correlator at 659 nm at a scattering angle of 90°. The sample of transmission electron microscope (TEM) was characterized by a high-resolution TEM (JEOL JEM-2100F) equipped with a CCD camera. Agilent cary eclipse fluorescence spectrophotometer, equipped a Cary single-cuvette peltier accessory, was used to steady-state fluorescence measurements recorded in a conventional quartz cuvette (light path 10 mm). A Ultraviolet-visible (UV-Vis) spectrophotometer (TU-1901, Beijing Purkinje General Instrument Co.,Ltd), equipped with a dual cuvette peltier accessory, was used to record UV-Vis absorbance in a quartz cuvette (light path 10 mm). The content of the IR783 in IR783-PEG-LPs and IR783-TR-LPs was

calculated according to the standard curve of free IR783. The loading content and encapsulation efficiency of IR783 were determined by:

IR783 loading content (%) = (weight of IR783 in LPs/weight of the whole LPs) ×100%

IR783 encapsulation efficiency (%) = (weight of IR783 in LPs/weight of total added IR783) ×100%.

Release of IR783 from IR783-PEG-LPs and IR783-TR-LPs at Different pH

Two phosphate buffered saline (PBS) buffers were adjusted to pH 6.5 and pH 7.4 by sodium hydroxide and hydrochloric acid, respectively. IR783-PEG-LPs or IR783-TR-LPs was added into a dialysis tubing (3.5K MWCO), which was carefully placed in a beaker (50 mL) containing above PBS buffer (20 mL). The temperature, stirring speed and working time of the heating plate were set to 37 °C, 200 rpm and 48 h, respectively. A sample (500 μL) was taken from the dialysate at regular intervals to measure the absorption spectrum. Finally, the released IR783 was measured by UV/vis absorption spectra according to the standard curve. After each sample, fresh PBS buffer (500 μL) was immediately added into the beaker to restore the original volume. Thus, the cumulative percentage of the released IR783 was calculated by:

The cumulative percentage of the released IR783 (%) = (Cumulative weight of released IR783 in dissolution medium)/Total weight of IR783 in IR783-PEG-LPs or IR783-TR-LPs) ×100%.

ROS generation measurements of IR783

The production of ROS from IR783 was monitored using DPBF as an ROS indicator based on degradation of DPBF, the absorption at 410 nm of DPBF reduced. In this experiment, a NIR laser source (λ = 808 nm) was performed at room temperature to examine the photophysical ability of IR783. As a control experiment, DPBF (50 μM) in dimethylformamide (DMF) absence IR783 was irradiated by a same NIR laser source. For DPBF itself, the absorbance of DPBF at 410 nm had no reduction observed in experimental time of irradiation, which indicated DPBF was stable under experimental conditions. Then, we examined the ROS generation of IR783 (10 μM) using DPBF (50 μM) in 2.0 mL of DMF. Upon irradiation (λ = 808 nm), the absorbance at λ=410 nm was

detected by UV-Vis spectroscopy within 100 seconds. Furthermore, vitamin C (VC), a ROS scavenger, was used to verify ROS production of IR783. Addition of VC (100 mM) with IR783 (10 μM) and DPBF (50 μM) in 2.0 mL of DMF, the absorbance at λ=410 nm was detected by UV-Vis spectroscopy within 100 seconds.

Photothermal properties of IR783-PEG-LPs and IR783-TR-LPs

The photothermal properties of IR783-PEG-LPs and IR783-TR-LPs and free IR783 aqueous solution under laser irradiation in Eppendorf tubes were determined with a thermal imaging camera (Fotric 225S). IR783-PEG-LPs and IR783-TR-LPs and free IR783 at different concentrations (0, 0.25, 0.5, 1.0 mM of IR783, 0.2 mL) were put into Eppendorf tubes and irradiated by the NIR laser (808 nm, 2 W/cm^2). Moreover, IR783-PEG-LPs and IR783-TR-LPs and free IR783 at fixed concentration of IR783 (0.5 mM, 0.2 mL) was put into Eppendorf tubes and irradiated by 808 nm laser (0, 1, 2, 3 W/cm^2). The temperature was automatically recorded every 30 seconds for 10 min.

Intracellular ROS detection

The generation of intracellular ROS was measured by laser confocal microscope (CLSM) using 2',7'-Dichlorodihydrofluorescein diacetate (DCFH-DA) as the ROS probe. After treating 4T1 cells with the IR783-PEG-LPs, IR783-TR-LPs and free IR783 (10 μM, the concentration of IR783) for 6 h in dark, the previous medium were replaced with fresh medium. DCFH-DA was added (final concentration of 10 μM) and incubate for 30 min. Subsequently, the cells were washed with PBS three times and further illuminated with a NIR laser (808 nm, 1 W/cm^2) for 2 min, followed by imaging with CLSM. The excitation light was selected to be 488 nm and the emission spectra in the wavelength range of 510-540 nm were collected by CLSM. Alternatively, before treatment with the IR783-PEG-LPs, IR783-TR-LPs and free IR783, the cells were pre-treated with N-acetylcysteine (1.0 mM) for 2 h. In addition, the IR783-PEG-LPs, IR783-TR-LPs and free IR783 nanoparticle-treated cells without laser irradiation, the cells with only laser irradiation, and the cells without any treatment were used as controls.

Intracellular PTT and PDT

Cell culture: Murine 4T1 breast cancer cells were incubated in DMEM medium with 10% FBS and 1% penicillin streptomycin at 37 °C in a humidified atmosphere containing 5% CO_2. Before experiments, the cells were pre-cultured until confluence was reached.

The cell viability of the IR783-PEG-LPs, IR783-TR-LPs and free IR783 against 4T1 cancer cells was evaluated by 3-(4,5-dimethylthiazol-2-yl)-2,5-diphenyl tetrazolium bromide (MTT) assay. In brief, 4T1 cells were seeded in 96-well plates at an appropriate density of 5×10^3 cells per well, respectively. After adherence, the 4T1 cancer cells were treated with IR783-PEG-LPs, IR783-TR-LPs and free IR783 (10 μM, the concentration of IR783) in the dark. After 6 hours of incubation, the previous medium was replaced with fresh medium. The cells were irradiated with a NIR laser (808 nm, 0.1 and 0.5 W/cm^2) for 2 min. Then, 100 μL of MTT solution (0.5 mg/mL) was added to each well and incubated for 4 h. Thereafter, the medium was removed and 100 μL of DMSO was added, followed by gently shaking for 10 min. The absorbance was measured at 490 nm using a microplate reader (Bio-Rad, iMark, USA). The relative cell viability was calculated as: cell viability = (OD490 (samples)/OD490 (control)) × 100%, where OD490 (control) was obtained in the absence of IR783-PEG-LPs, IR783-TR-LPs and free IR783, and OD490 (samples) was obtained in the presence of IR783-PEG-LPs, IR783-TR-LPs and free IR783. Each value was averaged from three independent experiments. As the control, the cytotoxicity of IR783-PEG-LPs, IR783-TR-LPs and free IR783 in the dark was also evaluated. Each value was averaged from three independent experiments.

In vivo imaging and antitumor study

In terms of animal and tumor models, all animal research were conducted in accordance with the guidelines established by the Guizhou Provincial Science Committee, and the entire project protocol was approved by the Animal Ethics Committee of Zunyi Medical University. Female BALB/c mice (5−6 weeks old) were bought from Vital River Laboratory Animal Technology (Beijing, China). The mice were used for in *vivo* fluorescence imaging and anti-tumor experiments. To establish the xenograft 4T1 tumor-bearing mouse model, 1×10^7 4T1 cancer cells were injected subcutaneously into the right side of the mouse. The mice with tumor volumes at around 100 mm^3 were used subsequently.

In *vivo* fluorescence imaging: The 4T1 tumor-bearing mice were intravenously administrated with 100 μL of IR783-PEG-LPs, IR783-TR-LPs and free IR783 solution (containing IR783: 1 $mg \cdot kg^{-1}$). Then the mice were anesthetized and imaged via a IVIS Lumina XRMS Series III system (PerkinElmer, MA, USA) at 0, 2, 4, 8 24 and 48 h post-injection. The excitation wavelength was 720 nm and in *vivo* spectral imaging from 790 to 850 nm (with 10 nm steps) was carried out. For the ex *vivo* tissues distribution study, the mice were sacrificed after 48 h injection, and tumor as well as major organs (heart, liver, spleen, lung, and kidney) were collected and subjected for ex *vivo* imaging.

In *vivo* photothermal imaging: To directly evaluate the photothermal effect of IR783-PEG-LPs, IR783-TR-LPs and free IR783 in *vivo*, Thermal imaging was applied to detect temperature changes in mice under NIR laser irradiation. The tumor-bearing mice were randomly divided into four groups of five mice each, and intravenously injected with IR783-PEG-LPs, IR783-TR-LPs and free IR783. The dose was adjusted at 1 mg/kg for IR783. As a control, mice were given the same volume of saline. The tumor-bearing mice treated with IR783-PEG-LPs, IR783-TR-LPs and free IR783 were irradiated with a NIR laser (808 nm, 0.5 W/cm^2) at 8 h post injection. Temperature changes and the IR images were acquired at 0, 1, 3, and 5 min.

For antitumor study, the tumor-bearing mice were randomly divided into four groups of five mice each: 1) "Saline", 2) "IR 783", 3) " IR783-PEG-LPs" 4) ", IR783-TR-LPs". The animals were intravenously administrated with saline, free IR 783 (1 $mg \cdot kg^{-1}$), IR783-PEG-LPs and IR783-TR-LPs (at dose of IR783 1 $mg \cdot kg^{-1}$), respectively, via the tail vein on day 0. Then, the mice were irradiated with a NIR laser (808 nm, 500 mW/cm^2) for 5 min at 8 h. The tumor size and body weight of the mice were measured every three days for 15 days. Tumor size was measured by a caliper and tumor volume was calculated using the following formula: $V = W^2 \times L/2$, where W and L were the shortest and longest diameters of tumors, respectively. Relative tumor size was calculated as V/V_0 (V_0 was the initial tumor volume). On day 15, all mice were sacrificed and the tumors were excised.

Acknowledgments

Not applicable.

Authors' contributions

ZLY and JG designed the experimental protocols. JJL carried out all the studies with help from TJL, MYY and MMW. JJL wrote the manuscript with help from ZLY and JG.

Funding

This work was supported by the Natural Science Foundation of China (Grant No. 82060626, 81360471), Innovative Group Project of Guizhou Province of Education (KY[2018]024), Guizhou Science and Technology Support Program([2020]4Y158), Talents of Guizhou Science and Technology Cooperation Platform [2020]4104. Cultivation project plan of new seedling cultivation and innovation exploration special project of Zunyi Medical University, Platform talents of Qiankehe, Grant/Award Number: [2018] No. 5772-030.

Availability of data and materials

All data generated or analyzed in this study are included in this article and its attached files.

Ethics approval and consent to participate

The use of animals was approved by and in accordance with the animal welfare committee of Zunyi Medical University.

Consent for publication

All authors agree to the publication of this study.

Competing interests

The author reports no conflicts of interest in this work.

Author details

[1]Key Laboratory of Basic Pharmacology of Ministry of Education and Joint International Research Laboratory of Ethnomedicine of Ministry of Education, Zunyi Medical University, Zunyi, Guizhou, 563003, China.

[2]Key Laboratory of Biocatalysis & Chiral Drug Synthesis of Guizhou Province, Zunyi, Guizhou 563003, P. R. China.

[3]School of Pharmacy, Zunyi Medical University, Zunyi, Guizhou 563003, P. R. China.

[4]Guizhou International Scientific and Technological Cooperation Base for Medical Photo-Theranostics Technology and Innovative Drug Development, Zunyi, Guizhou 563003, P. R. China.

Correspondence: Jie Gao and Ze-li Yuan

School of Pharmacy, Key Laboratory of Basic Pharmacology of Ministry of Education and Joint International Research Laboratory of Ethnomedicine of Ministry of Education Zunyi Medical University

No.6 West Xuefu Road, Zunyi, Guizhou 563003, P. R. China

Tel:+86-851-286-423-36

Fax:+86-851-286-432-36

E-mail: jiegao@mail.nankai.edu.cn; zlyuan@zmu.edu.cn

References

1. Luo DD, Carter KA, Miranda D, Lovell JF. Chemophototherapy: An Emerging Treatment Option for Solid Tumors. Adv Sci 2017.

2. Li X, Lee S, Yoon J. Supramolecular photosensitizers rejuvenate photodynamic therapy. Chem Rev. 2018;47:1174–88.
3. Li JC, Rao JH, Pu KY. Recent progress on semiconducting polymer nanoparticles for molecular imaging and cancer phototherapy. Biomaterials. 2018;155:217–35.
4. Gai SL, Yang GX, Yang PP, He F, Lin J, Jin DY, Xing BG. Recent advances in functional nanomaterials for light-triggered cancer therapy. Nano Today. 2018;19:146–87.
5. Sun H, Zhang Q, Li J, Peng S, Wang X, Cai R. Near-infrared photoactivated nanomedicines for photothermal synergistic cancer therapy. Nano Today. 2021;37:101073.
6. Fan W, Yung B, Huang P, Chen X. Nanotechnology for Multimodal Synergistic Cancer Therapy. Chem Rev. 2017;117:13566–638.
7. Gao J, Li J, Geng W-C, Chen F-Y, Duan X, Zheng Z, et al. Biomarker Displacement Activation: A General Host-Guest Strategy for Targeted Phototheranostics in Vivo. J Am Chem Soc. 2018;140:4945–53.
8. Liu YJ, Bhattarai P, Dai ZF, Chen XY. Photothermal therapy and photoacoustic imaging via nanotheranostics in fighting cancer. Chem Rev. 2019;48:2053–108.
9. Jung HS, Verwilst P, Sharma A, Shin J, Sessler JL, Kim JS. Organic molecule-based photothermal agents: an expanding photothermal therapy universe. Chem Soc Rev. 2018;47:2280–97.
10. Hong G, Antaris AL, Dai H. Near-infrared fluorophores for biomedical imaging. Nat Biomed Eng 2017.
11. Yoon H-J, Lee H-S, Lim J-Y, Park J-H. Liposomal Indocyanine Green for Enhanced Photothermal Therapy. ACS Appl Mater Interfaces. 2017;9:5683–91.
12. Zhang L, Yi H, Song J, Huang J, Yang K, Tan B, et al. Mitochondria-Targeted and Ultrasound-Activated Nanodroplets for Enhanced Deep-Penetration Sonodynamic Cancer Therapy. ACS Appl Mater Interfaces. 2019;11:9355–66.
13. Lim W, Jo G, Lee BY, Park MH, Hyun H. Rapid Clearance of IR783 and Methyl-β-cyclodextrin Complex for Improved Tumor Imaging. Part. Part. Syst. Charact. 2021;38:2100068.

14. Peer D, Karp JM, Hong S, Farokhzad OC, Margalit R, Langer R. Nanocarriers as an emerging platform for cancer therapy. Nat Nanotechnol. 2007;2:751–60.
15. Ruoslahti E, Pierschbacher MD. New perspectives in cell adhesion: RGD and integrins. Science. 1987;238:491–7.
16. Danhier F, Le Breton A, Préat V. RGD-based strategies to target alpha(v) beta(3) integrin in cancer therapy and diagnosis. Mol Pharmaceutics. 2012;9:2961–73.
17. Shi K, Long Y, Xu C, Wang Y, Qiu Y, Yu Q, et al. Liposomes Combined an Integrin αvβ3-Specific Vector with pH-Responsible Cell-Penetrating Property for Highly Effective Antiglioma Therapy through the Blood-Brain Barrier. ACS Appl Mater Interfaces. 2015;7:21442–54.
18. Li Y, Zhong D, Zhou C, Tu Z, Mao H, Yang J, et al. Sub-50 nm Supramolecular Nanohybrids with Active Targeting Corona for Image-Guided Solid Tumor Treatment and Metastasis Inhibition. Adv Funct Mater. 2021:2103272.
19. He T, He J, Younis MR, Blum NT, Lei S, Zhang Y, et al. Dual-Stimuli-Responsive Nanotheranostics for Dual-Targeting Photothermal-Enhanced Chemotherapy of Tumor. ACS Appl Mater Interfaces. 2021;13:22204–12.
20. Barua S, Mitragotri S. Challenges associated with Penetration of Nanoparticles across Cell and Tissue Barriers: A Review of Current Status and Future Prospects. Nano Today. 2014;9:223–43.
21. Li C, Greenwood TR, Bhujwalla ZM, Glunde K. Synthesis and characterization of glucosamine-bound near-infrared probes for optical imaging. Org Lett. 2006;8:3623–6.

Table 1 Characteristics of TR-LPs and PEG-LPs (n = 3)

Samples	pH	Diameter (nm)	Zeta potential (mV)	PDI	EE (%)	DL (%)
TR-LPs	6.5	104.4±2.0	+5.09±0.46	0.205±0.023	—	—
	7.4	143.3±1.1	-7.83±2.19	0.215±0.027	19.0±2.6	11.2±1.5
PEG-LPs	6.5	102.3±1.0	-18.15±4.48	0.209±0.011	—	—
	7.4	104.0±1.5	-16.00±0.84	0.163±0.003	21.8±1.5	14.8±2.6

Figure legends

Scheme 1 Schematic structure of IR783-TR-LPs.

Figure 1 Characteristics of TR-LPs. Size distribution (A) and TEM image of TR-LPs. Scale bar was 500 nm. (C) Size of TR-LPs changes with time in PBS buffer (pH 7.4), DMEM and 10% FBS. (D) UV−vis spectra and images of free IR783, IR783-PEG LPs and IR783-TR-LPs. (E) Photo-stability of free IR783, IR783-PEG LPs and IR783-TR-LPs under irradiation of LED light (white light, 6.78 W) at room temperature. (F) The cumulative percentage of IR783 released from IR783-TR-LPs at pH 6.5 and 7.4 (PBS buffer, 10 mM, 37 °C).

Figure 2 Phototheranostic properties of IR783-LPs. The photothermal properties of IR783-TR-LPs in PBS buffer at fixed IR783 concentration (0.5 mM) exposed to laser irradiation (0, 1, 2, 3 W/cm^2) (A) or at different IR783 concentration (0, 0.25, 0.5, 1 mM) exposed to NIR laser light (808 nm, 2 W/cm^2) (B) for 10 min. Photothermal imaging (C) and photothermal cycles (D) of IR783-TR-LPs. (E) The ROS generation of free IR783.

Figure 3 In *vitro* phototherapy evaluation. (A) Intracellular $^1O_2$ detection by CLSM after 4T1 cells were treated with the IR783-TR-LPs, IR783-PEG-LPs, free IR783 and DCFH-DA with 808 nm laser irradiation (1), no irradiation (2) and addition of N-acetylcysteine with 808 nm laser irradiation (3). Cells treated with DCFH-DA under irradiation (4) or dark (5) as control. Scale bar, 50 μm. (B) The cell viability of 4T1 cells were treated with the IR783-TR-LPs, IR783-PEG-LPs and free IR783 under different power of laser irradiation at pH 7.4. (C) The cell viability of 4T1

cells were treated with the IR783-TR-LPs, IR783-PEG-LPs and free IR783 under different power of laser irradiation at pH 6.5.

Figure 4 In *vivo* fluorescence and photothermal imaging. (A) In *vivo* fluorescence imaging of the 4T1 tumor-bearing mice at 2, 4, 8, 24 and 48 h after i.v. of IR783-TR-LPs, IR783-PEG-LPs and free IR783. Red cycles indicate the tumor sites. Ex *vivo* imaging of tumor and major organs harvested from the euthanized 4T1 tumor-bearing nude mice at 8 h post-injection. (B) In *vivo* photothermal imaging of the 4T1 tumor-bearing mice under laser irradiation (808 nm, 0.5 W/cm^2) at 1, 3 and 5 min (eight hours after intravenous injection).

Figure 5 In *vivo* PDT/PTT tumor ablation. (A) Changes of tumor volume in four groups. (B) Photos of the excised tumor. (C) Changes of body weight in four groups. (D) Histological sections of tumor tissues after treatment were stained with TUNEL and H&E, respectively. All scale bars are 100 μm. Error bars are based on standard error of mean (**$p < 0.05$).

Figure 6 IR783 encapsulated in TR-conjugated liposomes for enhancing NIR imaging-guided PTT and PDT

Figures

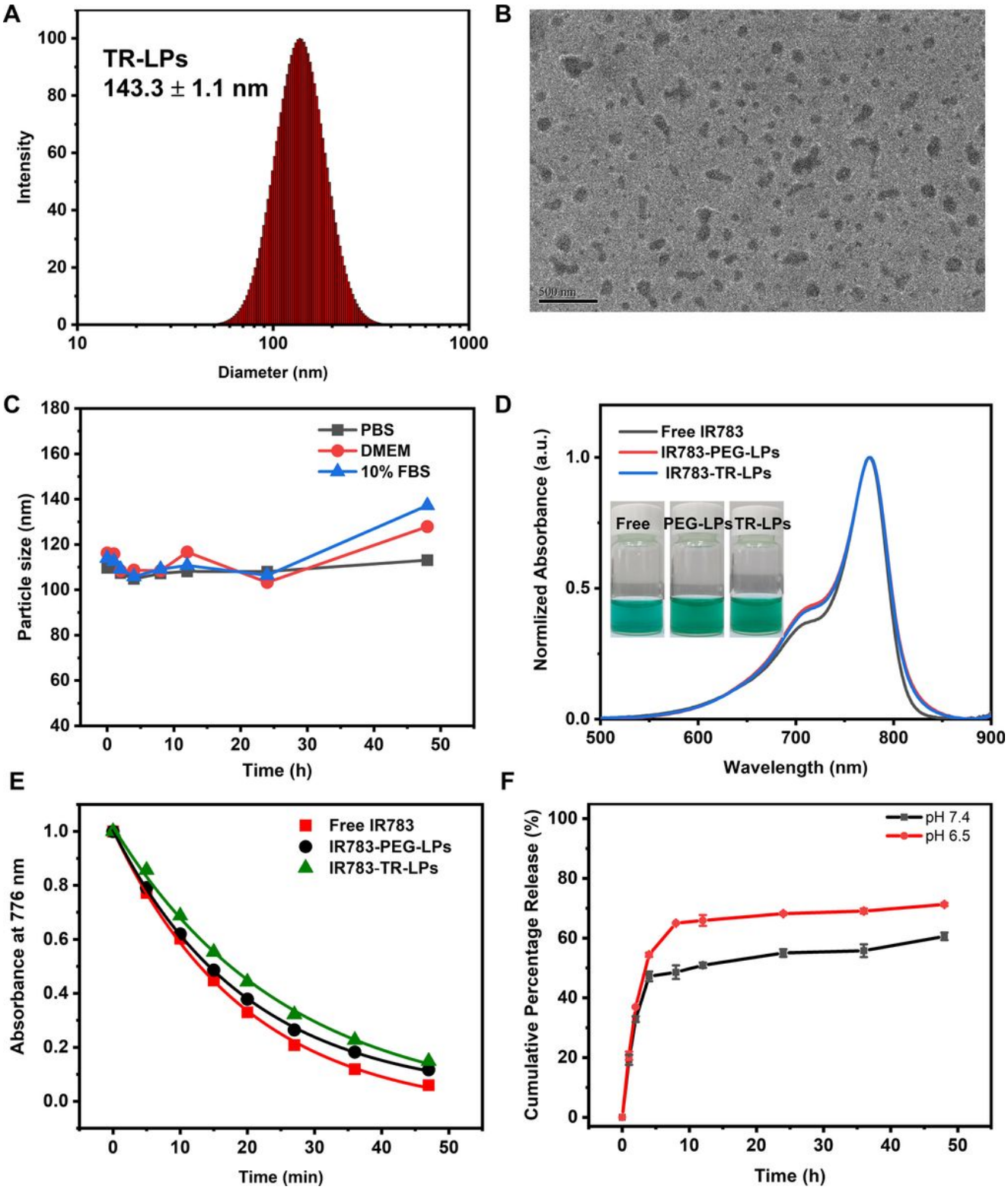

Figure 1

Characteristics of TR-LPs. Size distribution (A) and TEM image of TR-LPs. Scale bar was 500 nm. (C) Size of TR-LPs changes with time in PBS buffer (pH 7.4), DMEM and 10% FBS. (D) UV–vis spectra and images of free IR783, IR783-PEG LPs and IR783-TR-LPs. (E) Photo-stability of free IR783, IR783-PEG LPs

and IR783-TR-LPs under irradiation of LED light (white light, 6.78 W) at room temperature. (F) The cumulative percentage of IR783 released from IR783-TR-LPs at pH 6.5 and 7.4 (PBS buffer, 10 mM, 37 °C).

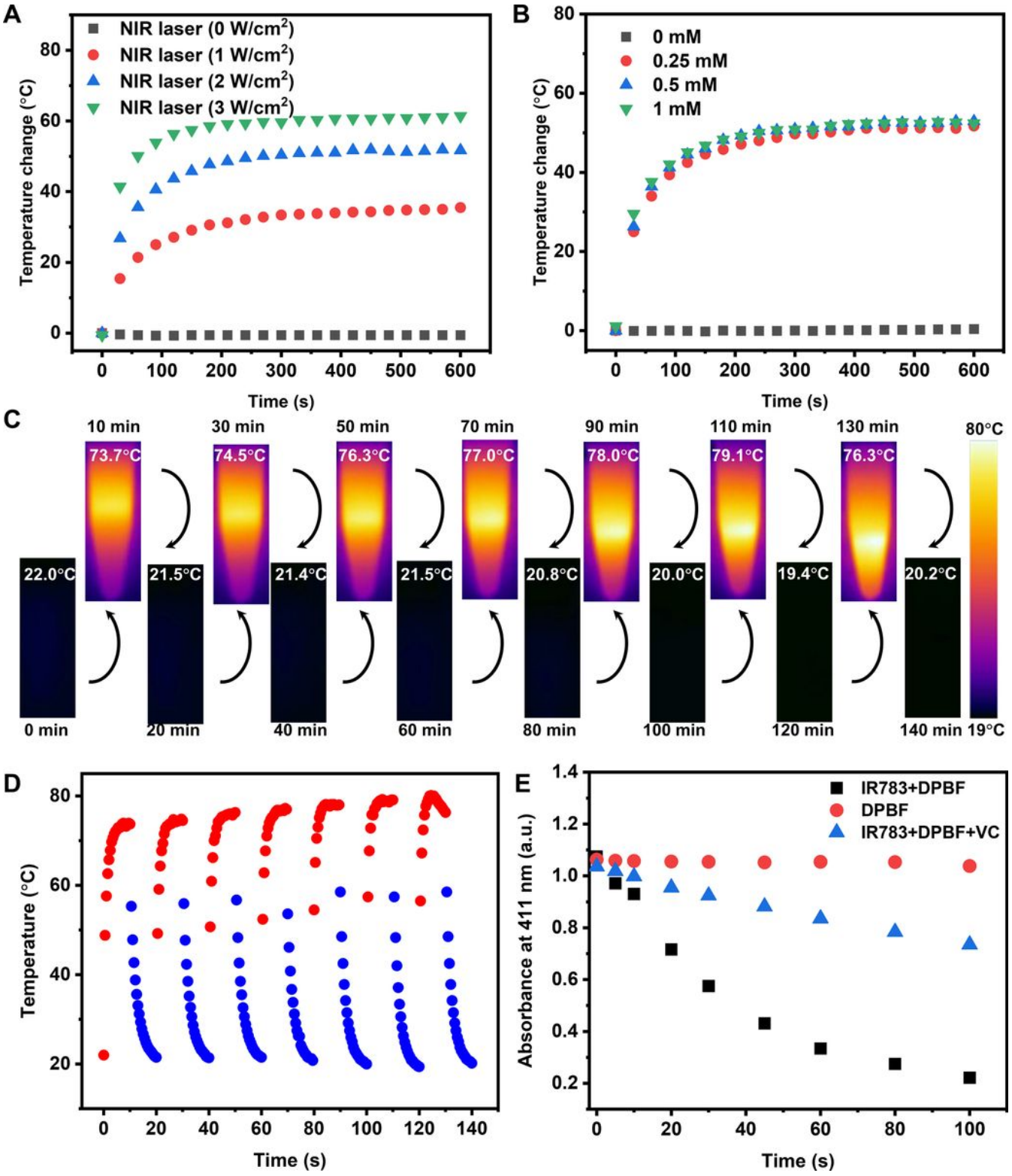

Figure 2

Phototheranostic properties of IR783-LPs. The photothermal properties of IR783-TR-LPs in PBS buffer at fixed IR783 concentration (0.5 mM) exposed to laser irradiation (0, 1, 2, 3 W/cm2) (A) or at different IR783

concentration (0, 0.25, 0.5, 1 mM) exposed to NIR laser light (808 nm, 2 W/cm2) (B) for 10 min. Photothermal imaging (C) and photothermal cycles (D) of IR783-TR-LPs. (E) The ROS generation of free IR783.

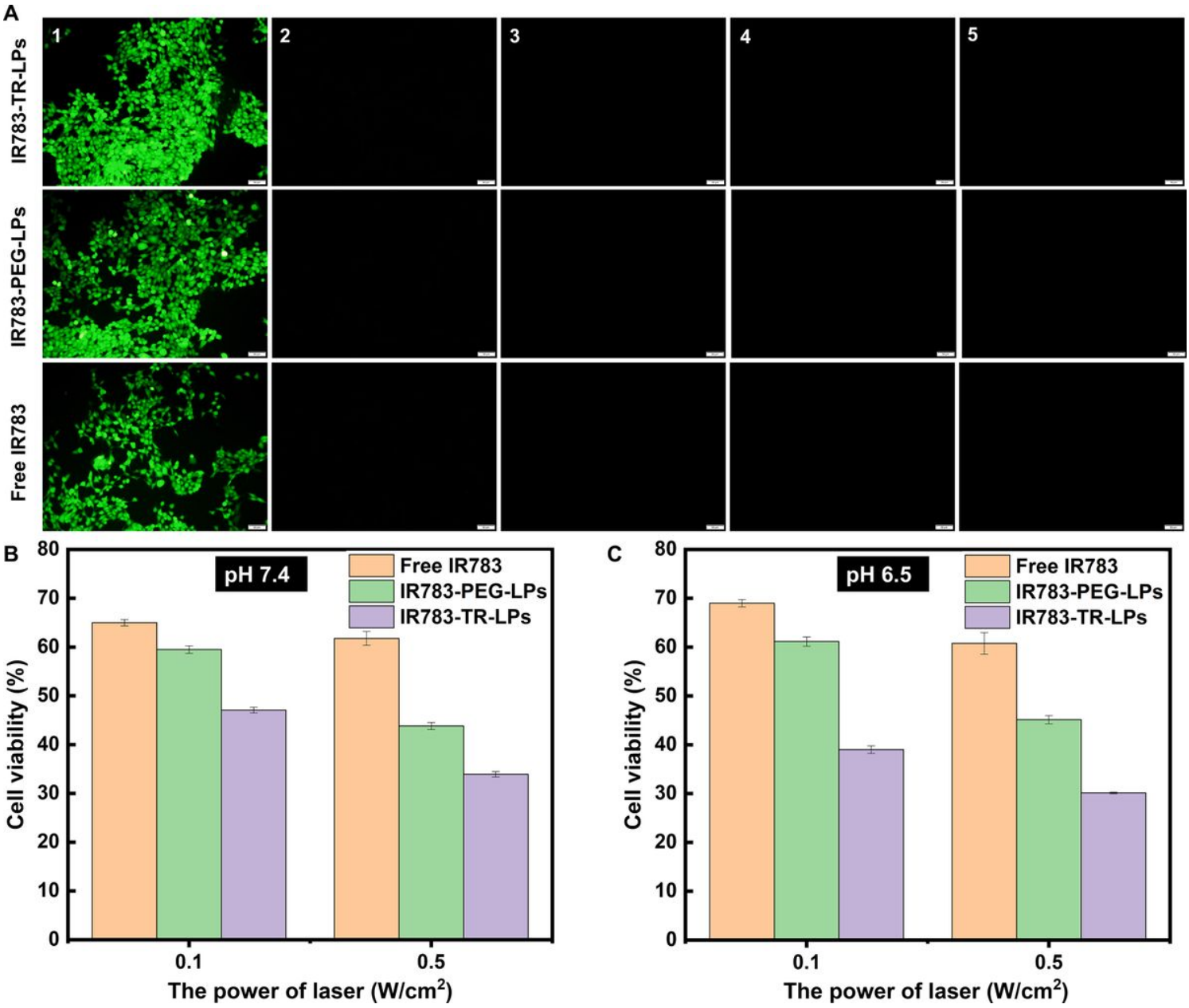

Figure 3

In vitro phototherapy evaluation. (A) Intracellular 1O2 detection by CLSM after 4T1 cells were treated with the IR783-TR-LPs, IR783-PEG-LPs, free IR783 and DCFH-DA with 808 nm laser irradiation (1), no irradiation (2) and addition of N-acetylcysteine with 808 nm laser irradiation (3). Cells treated with DCFH-DA under irradiation (4) or dark (5) as control. Scale bar, 50 μm. (B) The cell viability of 4T1 cells were treated with the IR783-TR-LPs, IR783-PEG-LPs and free IR783 under different power of laser irradiation at pH 7.4. (C) The cell viability of 4T1 cells were treated with the IR783-TR-LPs, IR783-PEG-LPs and free IR783 under different power of laser irradiation at pH 6.5.

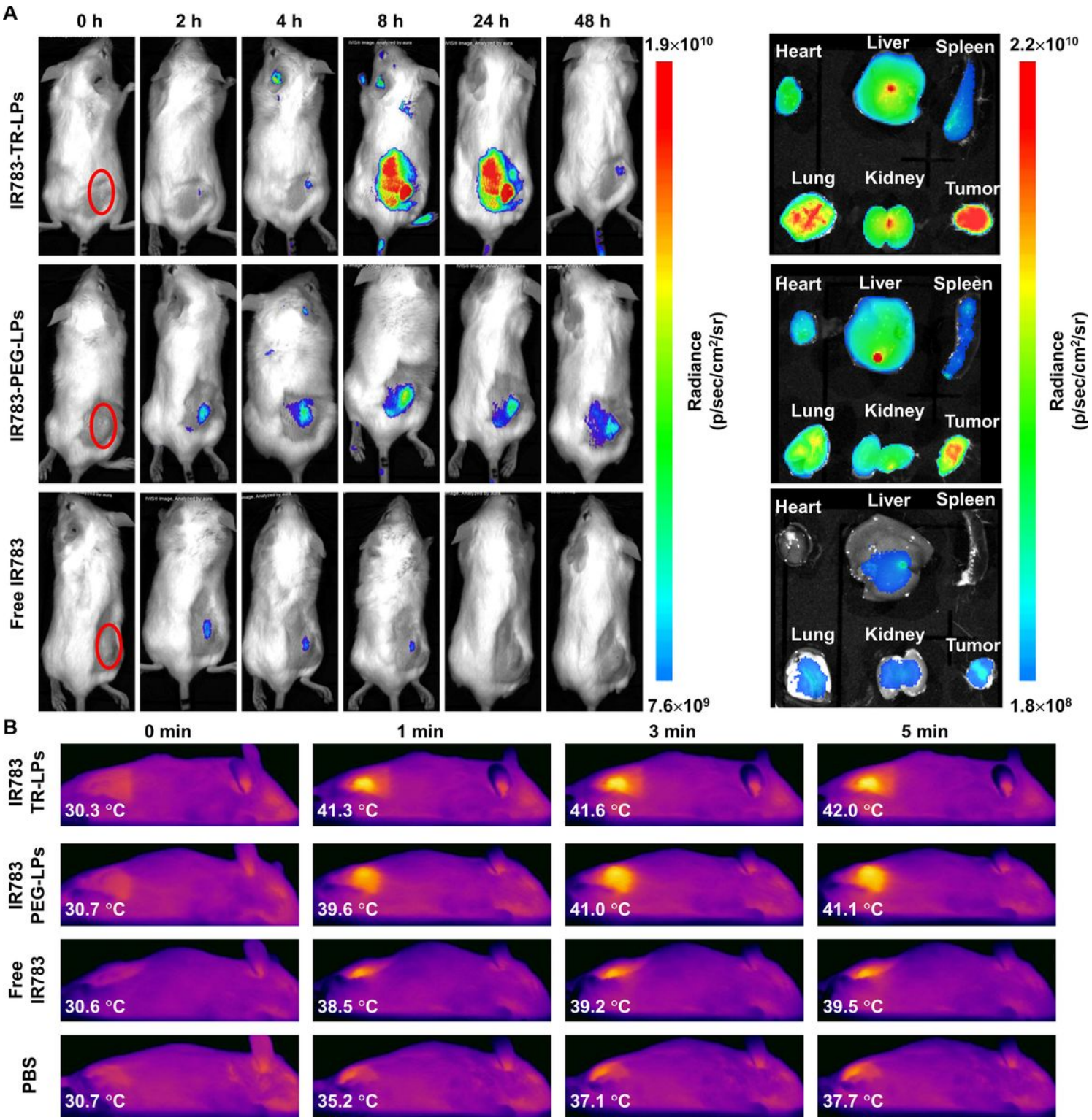

Figure 4

In vivo fluorescence and photothermal imaging. (A) In vivo fluorescence imaging of the 4T1 tumor-bearing mice at 2, 4, 8, 24 and 48 h after i.v. of IR783-TR-LPs, IR783-PEG-LPs and free IR783. Red cycles indicate the tumor sites. Ex vivo imaging of tumor and major organs harvested from the euthanized 4T1 tumor-bearing nude mice at 8 h post-injection. (B) In vivo photothermal imaging of the 4T1 tumor-bearing

mice under laser irradiation (808 nm, 0.5 W/cm2) at 1, 3 and 5 min (eight hours after intravenous injection).

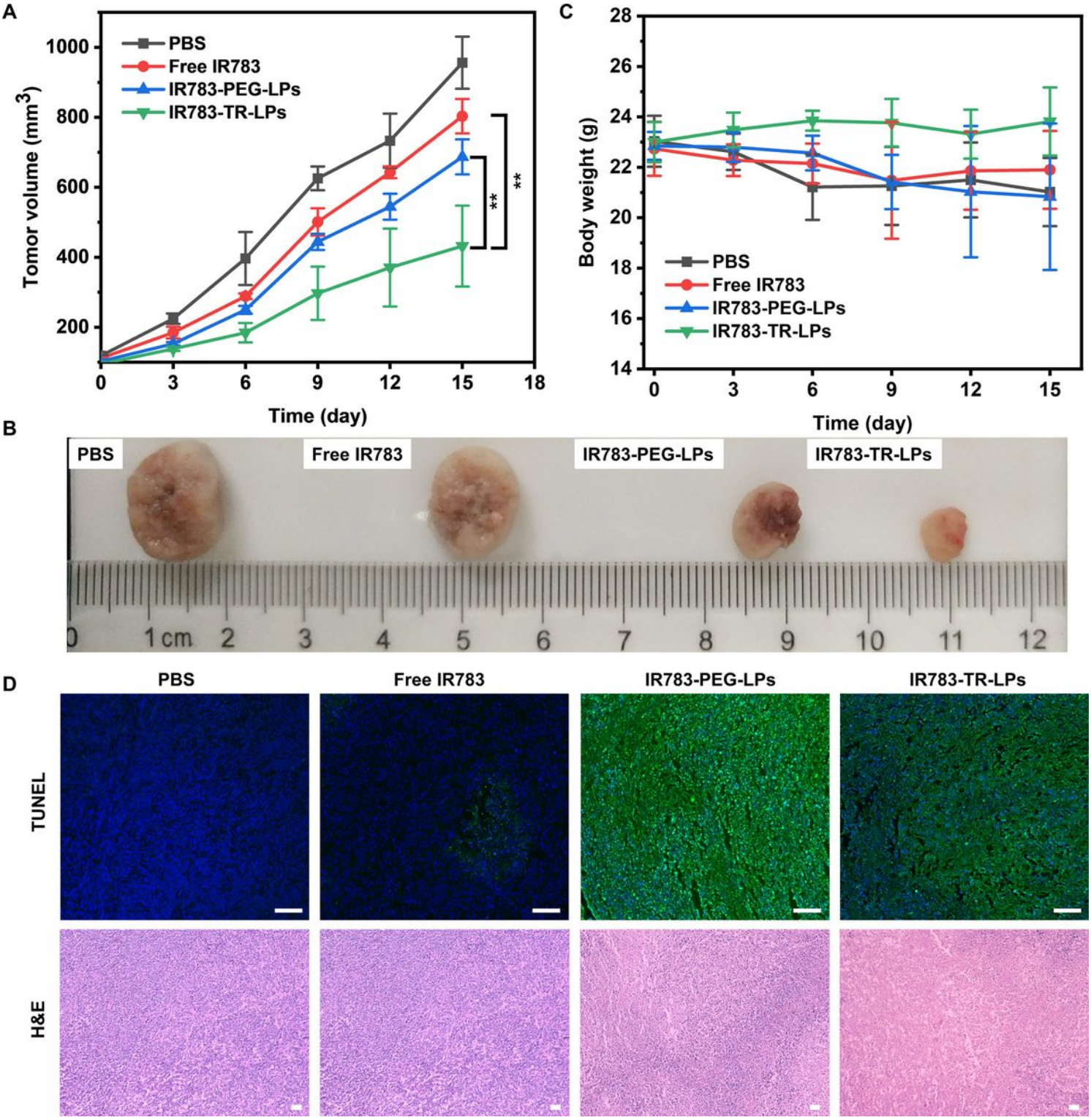

Figure 5

In vivo PDT/PTT tumor ablation. (A) Changes of tumor volume in four groups. (B) Photos of the excised tumor. (C) Changes of body weight in four groups. (D) Histological sections of tumor tissues after

treatment were stained with TUNEL and H&E, respectively. All scale bars are 100 μm. Error bars are based on standard error of mean (**p < 0.05).

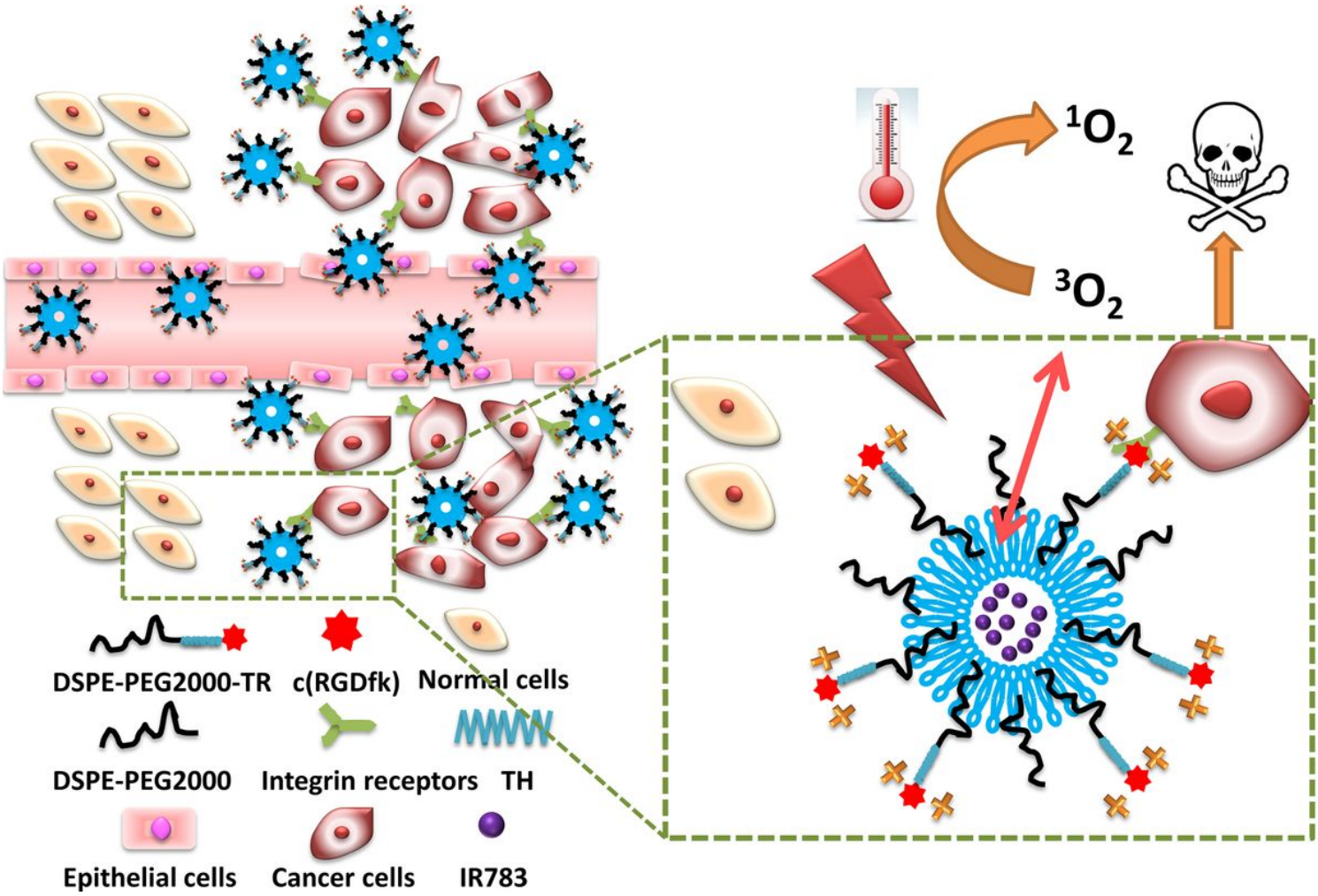

Figure 6

IR783 encapsulated in TR-conjugated liposomes for enhancing NIR imaging-guided PTT and PDT

Supplementary Files

This is a list of supplementary files associated with this preprint. Click to download.

- Scheme1.tif
- Supplementary.pdf
- GraphicalAbstract.jpg